

# **SRT Division: Architectures, Models, and Implementations**

David L. Harris, Stuart F. Oberman, and Mark A. Horowitz

Computer Systems Laboratory

Stanford University

Stanford, CA 94305

{harrisd, horowitz}@leland.stanford.edu, oberman@umunhum.stanford.edu

September 9, 1998

## Abstract

*SRT dividers are common in modern floating point units. Higher division performance is achieved by retiring more quotient bits in each cycle. Previous research has shown that realistic stages are limited to radix-2 and radix-4. Higher radix dividers are therefore formed by a combination of low-radix stages. In this paper, we present an analysis of the effects of radix-2 and radix-4 SRT divider architectures and circuit families on divider area and performance. Using analytical modeling and simulation, we evaluate the performance and area of a wide variety of divider architectures and implementations. We conclude that divider performance is only weakly sensitive to reasonable choices of architecture but is significantly improved by aggressive circuit techniques.*

## 1 Introduction

A simple and widely implemented class of division algorithm is digit recurrence. The most common implementation of digit recurrence division in modern microprocessors is *SRT* division, taking its name from the initials of Sweeney, Robertson [1] and Tocher [2], who developed the algorithm independently at approximately the same time. SRT division uses subtraction as the fundamental operator to retire a fixed number of quotient bits in each iteration. Two fundamental works on SRT division are those of Atkins [3], the first major analysis of SRT algorithms, and Tan [4], a derivation of high-radix SRT division and an analytic method of implementing SRT look-up tables. Ercegovac and Lang [5] provide a comprehensive treatment of the theory of SRT division and square root. Although division is typically an infrequent operation, ignoring its implementation significantly degrades system performance for many applications [6].

Various techniques have been proposed for increasing division performance, including cascading simple low-radix stages, overlapping sections of one stage with another stage, and prescaling the input operands [7]. All of these methods introduce area-performance tradeoffs. Ercegovac and Lang [5] analyze the tradeoffs of using several of these optimizations in the context of static CMOS standard-cells. Williams [8] presents a self-timed dynamic CMOS divider comprising a ring of five radix-2 stages that incorporates several of these techniques, and he also presents an analysis of the performance and area effects of the architectural components. Prabhu [9] presents the tradeoffs encountered when designing the Sun UltraSparc radix-8 divider.

In contrast to previous works, this paper analyzes in detail the effects of both circuit style and divider architecture on the performance and area of divider implementations. We present the performance results using the technology-independent metric of fanout-of-4 inverter delay. We therefore are able to extrapolate our results to future process technologies. While the discussion here is devoted to division, the theory of square root computation is an extension of the theory of division. Accordingly, most of the analyses presented here can also be applied to the design of square root units.

We survey the fundamental design parameters of SRT division and present the most common techniques for achieving higher performance in Section 2. Realizing the performance benefits of good circuit techniques, we examine circuit issues relating to dual-rail domino divider implementations in Section 3. Using the principles of logical effort, we develop in Section 4 an analytical model of divider speed that includes both intrinsic gate delays and the branching effort of parallel architectures. The model shows that some amount of quotient selection overlap is important, but that other architectural choices such as radix make little difference. Area and simulated performance results for a wide variety of divider architectures and circuit styles in Section 5 confirm the model's predictions. We conclude in Section 6 that fast SRT dividers should be built from domino circuits using any of several reasonable architectures to achieve speeds of 3.5-5 fanout-of-4 inverter delays per quotient bit.

## 2 Architectures

### 2.1 Definitions

Computer division by digit recurrence is similar to long division learned in elementary school. The partial remainder is initially set to the dividend. On each step, the divisor is compared to the partial remainder to produce a quotient digit. The quotient digit is multiplied by the divisor and subtracted from the partial remainder; the result is then shifted by one position to form a new partial remainder. Elementary school students use the quotient digit set  $\{0, \dots, 9\}$ , corresponding to radix 10. Computers often use radix 2 or radix 4. One step is required for each quotient digit. To analyze the latency of division, we must define the format of the operands and the range of each quotient digit.

In this analysis, the input operands are assumed to be represented in a normalized floating point format

with  $n$  bit significands in sign-and-magnitude representation. The algorithms presented here are applied only to the magnitudes of the significands of the input operands. Computing the resulting exponent and sign is straightforward. The most common format found in modern computers is the IEEE 754 standard for floating point arithmetic. This standard defines single and double precision formats, where  $n=24$  for single precision and  $n=53$  for double precision. The significand consists of a normalized quantity, with an explicit or implicit leading bit to the left of the implied binary point, and the magnitude of the significand is in the range  $[1,2)$ . However, to simplify the presentation, this analysis assumes fractional quotients normalized to the range  $[0.5,1)$ .

A division step which produces  $b$  bits of quotient is defined to be radix- $r$  where:

$$r = 2^b \quad (1)$$

Therefore, an  $n$  bit division using radix- $r$  requires  $k$  steps:

$$k = \frac{n}{b} \quad (2)$$

If each step takes one cycle, such an algorithm has a *latency* of  $k$  cycles. The *cycle time* of the divider is defined as the maximum time to compute one iteration of the algorithm. Depending upon the implementation, this may or may not be the same as the cycle time of the processor.

We can now formally define the steps of division. We set the initial partial remainder  $P_0$  to the dividend. On step  $j$ , we compute the next quotient digit  $q_{j+1}$  by comparing multiples of the divisor  $D$  to the current partial remainder:

$$q_{j+1} = SEL(P_j, D) \quad (3)$$

We then find the next partial remainder  $P_{j+1}$  by subtracting the selected divisor  $P_j$  multiple from the current partial remainder and shifting the difference:

$$P_{j+1} = r(P_j - q_{j+1}D) \quad (4)$$

The final quotient after  $k$  iterations is the weighted sum of the quotient digits:

$$q = \sum_{j=1}^k q_j r^{-j} \quad (5)$$

## 2.2 SRT Divider Parameters

To perform fast division, we would like an algorithm which has a low latency (in cycles) and a short cycle time. The latency is set by the radix  $r$ ; higher radices offer lower latencies. The cycle time is set by the operations occurring in each cycle: quotient digit selection and partial remainder generation. The simplest form of division, like that taught in elementary school, uses *nonredundant* quotient digits and partial remainder representations. This technique requires the quotient selection logic to exactly compare the partial remainder and divisor using a slow  $n$ -bit subtraction. An  $n$ -bit subtraction is also required to find the next partial remainder.

The key idea of SRT division is to guess the quotient digit based on a few of the most significant divisor and partial remainder bits, rather than computing it exactly. As long as the guess is close enough, the algorithm can correct on subsequent steps using *redundant* quotient digits. For example, a radix 2 quotient selection function could be built which guesses digits that are either correct or slightly too high. If a quotient digit set of  $\{-1, 0, 1\}$  instead of just  $\{0, 1\}$  is used, the  $-1$  digit can correct on a later step for an incorrect guess in a previous step.

Now quotient digit selection is faster because it only involves a few most significant bits rather than all  $n$ . To take advantage of this speedup, we must also improve partial remainder formation so that an  $n$ -bit subtraction is not required on each step. This can be done by keeping the partial remainder in redundant form such as  $P = P_s + P_c$ . The next redundant partial remainder can then be computed in a single gate delay using a (3,2) carry-save adder which sums  $P_s$ ,  $P_c$ , and  $-qD$ .

We will consider SRT division algorithms which use redundant quotient digits and partial remainder representations to avoid the slow  $n$ -bit subtractions. The two important divider parameters are the radix and the set of redundant quotient digits.

### 2.2.1 Choice of Radix

To minimize latency, as measured in cycles, we would like to use a high radix  $r$ . However, low latency does not come for free. As the radix increases, the quotient-digit selection becomes more complicated, which may increase the cycle time. Moreover, the generation of all required divisor multiples may become impractical for higher radices. Oberman [10] shows that the delay of quotient selection tables increases linearly with increasing radix, while the area increases quadratically. While prescaling of the input operands [11] reduces table complexity at the expense of additional latency, the difficulty in generating all divisor multiples for radix-8 and higher limits practical divider implementations to radix-2 and radix-4.

### 2.2.2 Choice of Quotient Digit Set

For a given choice of radix  $r$ , some range of digits is chosen for the allowed values of the quotient in each iteration. The nonredundant case is where, for radix  $r$ , there are exactly  $r$  allowed values of the quotient. However, to increase the performance of the algorithm, a *redundant digit set* is used. Such a digit set is composed of symmetric signed-digit consecutive integers, where the maximum digit is  $a$ . The digit set is made redundant by having more than  $r$  digits in the set. By using a larger number of allowed quotient digits, the complexity and latency of the quotient selection function is reduced because the later steps can correct for larger inaccuracies in the guess of the quotient digit. However, choosing a smaller number of allowed digits for the quotient simplifies generation of the multiples of the divisor. Specifically, for radix-2, the digit set is  $\{-1, 0, 1\}$ . For radix-4, there are two typical choices for the digit set: minimally redundant  $\{-2, -1, 0, 1, 2\}$  and maximally redundant  $\{-3, -2, -1, 0, 1, 2, 3\}$ . The quotient selection logic for a maximally-redundant radix-4 digit set is about 20% faster and 50% smaller than for a minimally-redundant digit set [10]. However, maximally-redundant radix-4 requires the computation of the 3x divisor multiple, which typically requires extra initial delay and area.

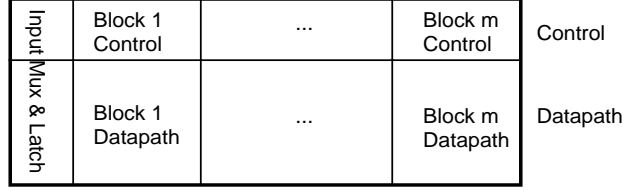


**Figure 1. SRT divider block diagram**

### 2.3 Higher Performance

Several techniques have been proposed for improving the performance of SRT division, but most involve cascading low-radix stages to form a higher radix divider. The primary problem with a cascade of stages is the proportional increase in cycle time. To avoid this increase, some computation can proceed in parallel at the expense of area. Taylor [12] proposes overlapping the quotient-digit selection of consecutive stages. Oberman [10] and Quach [13] discuss overlapping remainder computation. Fandrianto [14] discusses a cascade of lower radix segments in which there is no shifting of the partial remainder between the segments through the use of range reduction. In this study, we analyze the effects of five overlap schemes: no overlap, overlapped quotient selection, overlapped remainder computation, overlapped quotient and remainder computation, and a hybrid overlap scheme.

A general divider organization using overlapping is shown in Fig. 1. This floorplan is divided into a control section for quotient digit computation that typically operates on a small number of the most significant bits (about 4 for radix-2 and 8 for radix-4), and a datapath section for partial remainder formation of the remaining significand bits.

The divider is defined to comprise a cascade of  $m$  blocks, where each block has a delay of  $t_{block}$ . Each block is composed of  $s$  overlapped radix- $r$  stages. The divider therefore retires  $b' = m \times s \times b$  bits in each cycle, with a total cycle time of  $m \times t_{block} + t_{overhead}$ , where  $t_{overhead}$  includes latch delay, clock skew, and the input multiplexor for injecting new operands. Such an overlapped scheme produces  $k'$  radix- $r'$  digits with

$$r' = 2^{b'} \tag{6}$$

$$k' = \frac{n}{b'} \tag{7}$$

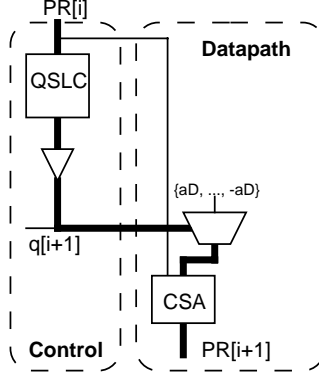


**Figure 2. Non-overlapped design**

The overlap schemes we consider are illustrated in Figs. 2 through 6. The critical path(s) are indicated by the heavy black lines. Although partial remainders are stored in carry-save form, they are drawn with a single line for simplicity. The architectures are shown overlapping two stages, but can be generalized to higher overlap [9].

### 2.3.1 Non-overlapped

A simple non-overlapped design is common in low-cost applications, such as the Intel Pentium Processor [15]. A block diagram is shown in Fig. 2. The quotient selection logic (QSLC) guesses the quotient digit  $q[i+1]$  based on the most significant bits of the current partial remainder  $PR[i]$  and the divisor. The result is buffered and driven across the datapath to select the appropriate divisor multiple, which is then subtracted from the partial remainder and shifted to form the next partial remainder  $PR[i+1]$ . Subtraction is performed in redundant form using the carry-save adder (CSA). Since the fixed shift involves only wire, the critical path delay is:

$$t_{block} = t_{qslc} + t_{buf} + t_{mux} + t_{csa} \quad (8)$$

### 2.3.2 Overlapping Quotient Selection

Overlapping quotient selection (Fig. 3) requires additional control logic but no additional datapath elements. This technique was demonstrated by Taylor [12]. The critical path involves speculatively gener-



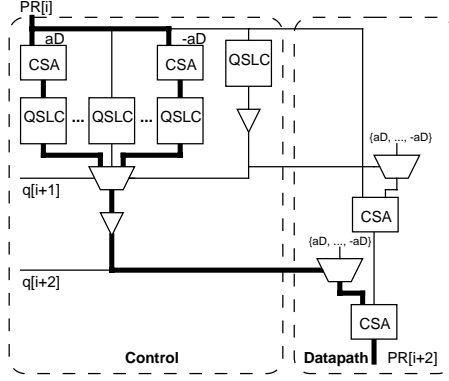


Figure 3. Overlapped quotient selection

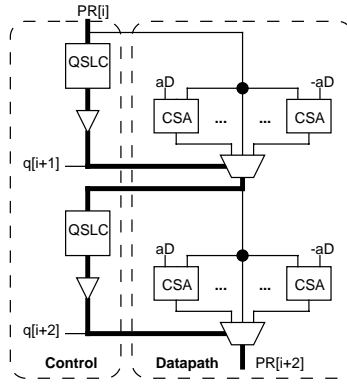


Figure 4. Overlapped remainder formation

ating all possible second quotient digits, then choosing among them given the first quotient digit. The results are used to select the appropriate divisor multiple to subtract from the partial remainder. The datapath CSAs may be optimized for a single late input. The critical path for  $s = 2$  is to:

$$t_{block} = t_{qslc} + t_{buf} + 2t_{mux} + 2t_{csa} \quad (9)$$

### 2.3.3 Overlapping Remainder Formation

Overlapping partial remainder computation (Fig. 4) speculatively computes all of the next partial remainders, then selects the appropriate one based on the actual quotient digit. The critical path delay for  $s = 2$  is:

$$t_{block} = 2(t_{qslc} + t_{buf} + t_{mux}) \quad (10)$$

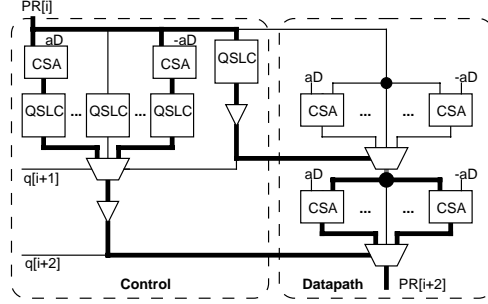


Figure 5. Overlapped remainder and quotient selection

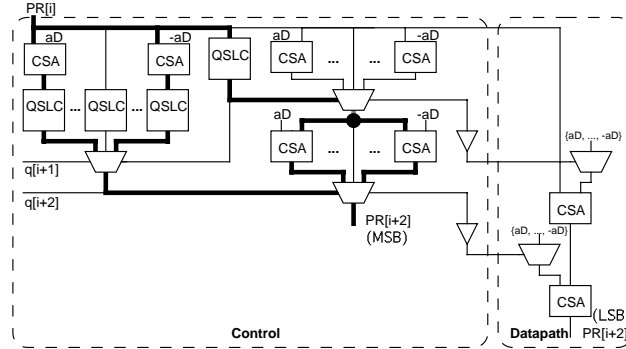


Figure 6. Hybrid overlapping

### 2.3.4 Overlapping Quotient Selection and Remainder Formation

The previous two schemes can be combined (Fig. 5) such that both the quotient selection and partial remainder formation are overlapped. The Sun UltraSparc [9] implements such a combination. This design has two equally critical paths, one through the quotient digit selection logic, and the other through the speculative partial remainder formation. The critical path delay for  $s = 2$  is:

$$t_{block} = t_{qslc} + t_{buf} + 2t_{mux} + t_{csa} \quad (11)$$

### 2.3.5 Hybrid Overlap

Closer examination shows that only the most significant bits of the next partial remainder are critical. We can exploit this fact in two ways. One is to buffer the quotient digits before driving the low-order mux selects. This optimization is applicable to all architectures. Another is to only overlap partial remainder formation of the critical high-order bits to save area. These techniques are combined in Fig. 6.

This architecture is a hybrid of the overlapped quotient selection and remainder formation design for the critical bits and the overlapped quotient selection design for the non-critical bits. The quotient digits are buffered before driving the non-critical least significant bits in the datapath. This eliminates the buffer delay from the critical path to the high order bits. The critical path delay for  $s = 2$  is:

$$t_{block} = t_{qslc} + 2t_{mux} + t_{csa} \quad (12)$$

Hardware is saved relative to designs which overlap partial remainder formation because no speculative adders are needed in the datapath for partial remainder formation. The non-critical partial remainder bits lag behind the critical bits by the delay of a buffer plus CSA. This may slightly increase the time required for rounding and normalization at the end of a divide. More importantly, the non-critical bits must catch up before they are required by quotient selection. Therefore, the speculative partial remainder formation must operate on  $s \times b$  extra bits to catch these bits up before they become critical. The lag of the non-critical bits plus the delay through the partial remainder formation must be less than the delay of the critical quotient selection path so that the non-critical bits catch up as they are shifted into the critical portion. Specifically, the critical path delay from  $q[i+2]$  to  $PR[i+4]$  through the quotient digit logic to generate the next set of most-significant partial remainder bits is:

$$t_{crit} = t_{mux} + (t_{csa} + t_{qslc} + t_{mux} + t_{mux}) \quad (13)$$

while the sum of the lagging path delay and partial remainder formation delay is:

$$t_{noncrit} = (t_{buf} + t_{mux} + t_{csa}) + (t_{csa} + t_{mux} + t_{csa} + t_{mux}) \quad (14)$$

Simplifying, to keep  $t_{noncrit} < t_{crit}$ ,

$$t_{buf} + 2t_{csa} < t_{qslc} \quad (15)$$

Architecture	Block Latency	# QSLC	# Wide CSAs	# Wide MUXes	# Bitlines
Non-overlapped	$s(t_{qsel} + t_{buf} + t_{mux} + t_{csa})$	$s$	$s$	$s$	$5 + a$
Overlap PR	$s(t_{qsel} + t_{buf} + t_{mux})$	$s$	$2as$	$s$	$6 + a$
Overlap QS	$t_{qsel} + t_{buf} + st_{mux} + st_{csa}$	see Table 2	$s$	$s$	$5 + a$
Overlap PRQS	$t_{qsel} + t_{buf} + st_{mux} + (s - 1)t_{csa}$	see Table 2	$2as$	$s$	$6 + a$
Hybrid overlap	$t_{qsel} + st_{mux} + (s - 1)t_{csa}$	see Table 2	$s$	$s$	$5 + a$

**Table 1. Comparison of architectures**

As we show later, quotient selection is the most time consuming component, especially for radix-4 designs. Therefore, it is reasonable to expect this constraint to be satisfied, especially since the datapath CSA may be optimized for a single late input. If quotient selection is too fast, the final partial remainder formation can be overlapped in the datapath, adding more CSAs, but relaxing the timing constraint from Eq 15 to  $t_{buf} + t_{csa} < t_{qslc}$ .

## 2.4 Comparison

Table 1 compares the latency, hardware cost, and wiring of each architecture. The number of QSLCs, which dominate control area, and number of CSAs and MUXes in the datapath are listed. Also, the number of metal tracks required is computed (see Fig. 7). Overlapping quotient digit selection saves  $s - 1$  quotient selection and buffer delays at the expense of additional quotient selection logic blocks. Overlapping partial remainder formation saves the delay of one CSA at the expense of many more CSAs performing speculative computation. Finally, the hybrid scheme eliminates the buffer delay and also avoids a large number of speculative CSAs. From Table 1, the hybrid overlapping scheme has the lowest latency and also saves hardware relative to the next fastest scheme. However, the performances of other architectures that overlap quotient selection are within a CSA and buffer delay of the hybrid scheme, and as discussed previously, the buffer may be optimized out of the critical path.

The number of quotient selection blocks increases sharply when moving from radix-2 to radix-4 and for increasing  $s$ , as shown in Table 2. Due to the exponential area increase with degree of overlap, reasonable designs are limited to an overlap of  $s = 2$  or possibly  $s = 3$ .

$s$	$r = 2 \ a = 1$	$r = 4 \ a = 2$	$r = 4 \ a = 3$
1	1	1	1
2	4	6	8
3	11	27	39
4	26	112	166

**Table 2. QSLCs for overlapped architectures**

### 3 Circuits

Overlapping stages is important, but Table 1 shows that the incremental improvement of better overlap techniques is small. Execution unit designers are therefore turning to more aggressive circuit techniques, especially domino circuits, to greatly reduce latency [16].

Three key circuit issues which impact architectural choices are domino monotonicity requirements, wiring cost, and clocking overhead. Designers accustomed to static logic must remember that domino circuits require monotonically rising inputs during evaluation. Since single-rail domino circuits are not a functionally complete logic family, non-monotonic gates such as CSAs require dual-rail inputs and outputs to code both true and complementary signals. This increases the area of logic gates and the amount of interconnect. Radix-4 quotient selection logic is especially impacted because it is relatively large. Fortunately, the quotient digits are consumed only by multiplexors, so they can be computed in single-rail 1-hot form. Two options for fast QSLCs are domino gates and dynamic self-timed PLAs. We found that radix-4 minimally/maximally redundant 1-hot PLAs have 50/25 minterms respectively, while according to [10] minimally/maximally redundant Gray-encoded PLAs have only 25/14 minterms. Static designs can implement either a 1-hot PLA or an encoded PLA to save area, but domino implementations require the larger 1-hot design.

The datapath dominates the area of most dividers, so we must examine the number of bitlines running between elements within a bitslice. Dynamic designs double the wire count because dual-rail signals are needed. All floating point blocks have fixed overhead of power, ground, and three data busses: two inputs and one output. Dividers have many additional bitlines because partial remainders are kept in redundant form.

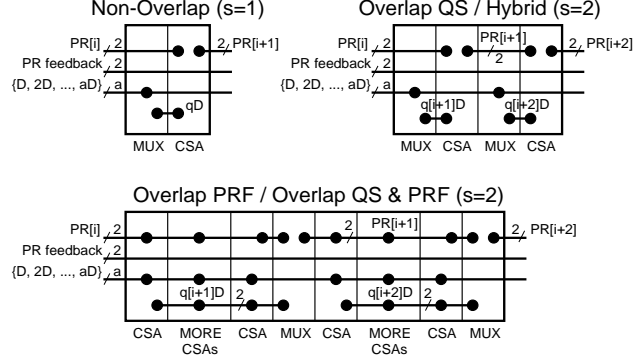


**Figure 7. SRT datapath floorplan for one block**

Fig. 7 illustrates wiring requirements on a floorplan of a block for various architectures. A dot on a wire over an element indicates that the signal is used in that element. On all architectures, two lines are required for driving the redundant partial remainder along the path and another two lines are required for feeding the result back to the next iteration. Furthermore, divisor multiples must be driven to all of the blocks. Although there are  $2a + 1$  divisor multiples, we must only transmit the  $a$  positive multiples and can generate the negative multiples with a local inversion. Finally, the appropriate divisor must be selected. In architectures which do not speculatively generate partial remainders, only one wire is required to drive the divisor mux output to the CSA which generates the next partial remainder. In speculative architectures,  $2a$  CSAs generate two bits of output each. It would seem  $4a$  wires are required as input to the divisor mux. However, by distributing the multiplexor legs across the adders, only two wires are needed for the redundant result.

A static divider requires either  $5 + a$  or  $6 + a$  bitlines, which poses little difficulty. A dual-rail domino divider requires twice as many bitlines. These bitlines can be accommodated in a bit pitch of about  $120\lambda$ , where  $\lambda$  is half of the minimum drawn transistor length. Cells can be efficiently laid out at this pitch, so wire limitations are not expected to increase divider area significantly in a process with 3 or 4 metal layers. This is consistent with [8] which reports only a 15% area penalty for dual-rail domino in a 2 layer process.

Clocking overhead is important in both static and dynamic designs. Static designs conventionally use a flip-flop with a multiplexor at the beginning of the cycle to capture either a new divider input or the result of the previous iteration. The flip-flop adds a delay of  $t_{clk \rightarrow q} + t_{setup} + t_{skew}$  to the path, which

can be large. Textbook domino designs require latches between phases of domino logic and are also sensitive to clock skew, but skew-tolerant domino techniques [17] make domino much more attractive by eliminating latch delays and clock skew from the critical path. Good domino designs must only pay the cost of one 2:1 multiplexor at the beginning of each cycle. This cost may be amortized over many bits produced in the cycle.

Since the area is proportional to the number of blocks, area can be reduced without impacting latency by clocking the divider at a higher frequency than the rest of the processor. For example, the HP-PA7100 [18] achieves higher radix by clocking a lower radix core at double frequency. This technique improves area at the expense of the complexity of generating a higher frequency clock.

In summary, domino is an attractive approach for high-performance dividers. It greatly reduces gate delays and eliminates much of the clocking overhead found in flip-flop-based static designs. The domino wiring requirements do not significantly increase area in processes with 3 or more metal layers. Thus, the primary costs of domino designs are the extra area consumed by quotient selection logic, the increased power consumption while the divider is active, and the necessary circuit design expertise.

## **4 An Analytical Model for Divider Delay**

The analysis of architectures explores the elements in each critical path and suggests that certain architectures may be faster than others because they have fewer gates in the critical paths. However, critical path delay is a strong function of the loading each gate must drive as well as the number of gates. This section develops a more powerful model based on the principles of logical effort to compare the delay of dividers. The model is calibrated with simulations of a few building blocks and predicts the performance of a wide variety of architectures. An important limitation of the model is that it neglects wiring capacitance and thereby underestimates the delay of highly parallel architectures with lengthy wires.

## 4.1 Logical Effort

The delay of a CMOS gate depends on the intrinsic delay of the gate driving its internal parasitics, on the load that must be driven, and on the effective resistance of the gate. This can be modeled as:

$$t = t_{int} + rf \quad (16)$$

where  $t_{int}$  is the intrinsic delay,  $f$  is the fanout, defined as  $C_{load}/C_{in}$ , and  $r$  is proportional to the effective resistance of the gate. More complex gates have larger  $t_{int}$  and  $r$  terms.

Sutherland [19] defines the logical effort  $LE$  of a gate to be the ratio of its effective resistance to that of an inverter with the same input capacitance. The gain  $g$  of the gate can then be defined as the fanout multiplied by the logical effort. Now the delay can be rewritten in terms of the gain of each gate.

$$LE = r_{gate}/r_{inv} \quad (17)$$

$$g = LE \cdot f \quad (18)$$

$$t = t_{int} + gr_{inv} \quad (19)$$

The gain  $G$  of an entire path is the product of the gains of each stage. This gain comes from the logical effort of each stage, the overall fanout of the path, and any branching within the path. The overall fanout  $F$  is defined as  $C_{load}/C_{in}$  of the path. The branching factor  $B$  accounts for other loads within the path; for example, a path from computing a multiplexor select to the data output of one bit of a 64 bit mux has  $B = 64$  because 63 other multiplexor bits must be driven. In summary, a path with  $\sigma$  stages has:

$$G = BF \prod_{i=1}^{\sigma} LE_i \quad (20)$$

It can be shown that the delay of a path is minimized when gates are sized such that each stage has equal gain. The minimum path delay therefore is the sum of the gain-dependent delay, which is equal



per stage, plus the intrinsic delays of each stage.

$$t_{path} = \sigma r_{inv} \sqrt[\sigma]{G} + \sum_{i=1}^{\sigma} t_{int-i} \quad (21)$$

## 4.2 Critical Paths

The delay of various architectures can now be modeled using the logical efforts and intrinsic delays of each stage and the branching effort and fanout of the path. Since each divider block drives an identical divider block, path fanout is always 1 and will be ignored. This section analyzes architectures to find the components in the critical path and the overall branching effort of the path. The next section describes simulations used to extract logical efforts and intrinsic delays of each component.

The delay of CSAs and multiplexors depends on which inputs are critical. A CSA with a single critical input can be fast if the sum and carry results are speculatively computed for both possible values of the critical input, then simply selected when the critical input arrives. A CSA with two critical inputs cannot use this optimization. Similarly, a multiplexor can be optimized for late control inputs, late data inputs, or simultaneously arriving control and data. To capture these optimizations, elements are defined as CSA1, CSA2, MUXC, MUXD, and MUXB, corresponding to CSAs with 1 and 2 late inputs and multiplexors that are control-critical, data-critical, or both control and data critical.

Branching effort of a path depends on operand width,  $n$ , range of quotient digits,  $a$ , and amount of overlapping,  $s$ . Although overlapped architectures compute with slightly more than  $n$  bits,  $n$  is a convenient and simple estimate. Consider the fanout of each architecture in more detail.

Non-overlapped dividers have branching effort of  $n$  to drive the divisor selection mux in the datapath.

Dividers using overlapped partial remainder formation have a branching effort of  $n$  each time the quotient bit drives the divisor selection mux. Thus, overlap by two has a branching effort of  $n^2$ .

Dividers using overlapped quotient selection have a branching of  $n$  driving the divisor selection mux, times additional branching as PR[i] drives speculative quotient selection logic. Assuming non-critical gates can be buffered sufficiently to present negligible load, each level of speculative quotient selection

Architecture	$s$	B	QSLC	CSA2	CSA1	MUXC	MUXD	MUXB	BUF
Non-overlapped	1	$n$	1		1	1			1
Overlap PR	2	$n^2$	2			2			2
Overlap QS	2	$2an$	1	1	1	1	1		1
Overlap QS	3	$4a^2n$	1	2	1	1	2		1
Overlap PRQS	2	$2an(2a + 1)$	1	1		1		1	1
Hybrid overlap	2	$2az(2a + 1)$	1	1		1		1	

**Table 3. Branching effort and component count of divider architectures**

involves branching of roughly  $2a$ . Therefore, for overlap of  $s$  the total branching effort is  $(2a)^{s-1}n$ , which reduces to the non-overlapped case for  $s=1$ .

Dividers using both overlapped partial remainder and quotient logic with  $s = 2$  have three sources of branching. Branching of  $2a + 1$  occurs as PR[i] drives the speculative and non-speculative quotient selection logic. Another branching of  $n$  occurs when the q[i+1] signal drives the divisor selection mux. Finally, a branching of  $2a$  occurs as PR[i+1] drives the speculative partial remainder formation CSAs. Total branching effort is therefore  $2an(2a + 1)$ .

Hybrid overlap with  $s = 2$  is identical to the case of overlapped partial remainder and quotient logic except that the branching of  $n$  driving divisor selection muxes is reduced to branching of  $z$  driving only a few of the most critical bits.  $z$  is the number of bits used in the control block; typical values are 6 for radix 2, 10 for maximally redundant radix-4, and 11 for minimally redundant radix-4. Total branching effort is therefore  $2az(2a + 1)$ .

Table 3 summarizes the branching effort and number of each component in the critical path of various architectures.

### 4.3 Calibrating the Model

Using these component counts and fanouts, the logical effort model can predict the delay of dividers. The  $LE$  and  $t_{int}$  terms in the model can be estimated by hand or measured from simulation. Table 4 lists the terms based on simulation of domino gates in the HP-CMOS26B 1  $\mu\text{m}$  (drawn) process. To normalize for process, all times are expressed as multiples of the delay of a fanout-of-4 (FO4) inverter.

Component	$LE$	$t_{int}$
CSA1	1.22	0.58
CSA2	2.16	1.05
MUXC3	0.59	0.66
MUXD3	0.61	0.72
MUXB3	0.92	0.78
MUXC5	0.59	0.76
MUXD5	0.62	0.82
MUXB5	0.93	0.88
MUXC7	0.60	0.85
MUXD7	0.63	0.91
MUXB7	0.94	0.98
BUF	0.41	0.35

**Table 4. Component logical efforts and intrinsic delays**

Note that each domino gate actually consists of a dynamic gate and a static inverter, each of which may be sized for best performance. Therefore, the domino gate counts as two stages when allocating gain per stage. Also note that multiplexor delays depend on the number of inputs  $2a + 1$ .

Computing the logical effort of quotient select logic would be awkward because the QSLC consists of many stages of logic. Instead, a QSLC block is designed with an overall  $C_{out}/C_{in}$  of 1 and simulated to produce an absolute delay. Therefore, the block can be modeled as a fixed delay, contributing nothing to the gain-dependent delay of the path. The radix-2 QSLC is built from two complex domino gates. The radix-4 QSLCs are built from short carry-propagate adders to sum the most significant redundant partial remainder bits, followed by a dynamic PLA computing a 1-hot quotient digit. Table 5 lists the QSLC delays for radix-2 and radix-4 designs. For radix-4, the adder and PLA components of the delay are listed explicitly. PLA delay was obtained through simulation, while the 10 or 8 bit adder delay was estimated from data in Section 5.

#### 4.4 Model Results

Table 6 lists the delays of divider architectures estimated with the logical effort model. The  $t_{int}$  column contains the sum of the intrinsic delays through each stage, including the QSLC. The  $B$  column

	$r = 2 \ a = 1$	$r = 4 \ a = 2$	$r = 4 \ a = 3$
$t_{PLA}$	n/a	4.3	3.8
$t_{add}$	n/a	4.6	4.0
$t_{QSLC-total}$	3.2	8.9	7.8

**Table 5. Fanout-of-1 quotient select delays**

lists the total branching effort of a block. The  $G$  column lists the total gain of a block. The  $\sigma$  column lists the number of stages in the block. As mentioned earlier, each domino gate represents two stages and QSLCs are modeled as a fixed delay contributing no stages of gain. The  $t_{block}$  column shows the total delay obtained from Eq 21. Finally, the table shows the number of quotient bits each block produces and the overall delay per bit.

#### 4.5 Conclusions

The analytical delay model provides a simple way to compare many divider architectures. It is more powerful than merely counting gates in the critical path because it also accounts for the fanout of the gates. The model shows that some amount of overlapping quotient selection is important for good performance. As long as quotient selection is overlapped, other architectural choices make little difference in performance.

Two limitations of the model are that it includes neither wiring delay nor 3x divisor multiple generation. For non-overlapped designs, the only long wires are the ones which drive select lines across the datapath and have delays dominated by gate loading. Designs with overlapped quotient selection add long wires to distribute the speculative quotient bits and most significant partial remainder bits around the QSLCs. These wire lengths increase exponentially with  $s$  and thus contribute to heavier loadings than predicted for overlapped architectures. Radix-4 maximally redundant divider delays also are longer than predicted because time is required in advance for 3x divisor multiple generation.

The consequence of these limitations is that the architectures predicted to be fastest are those for which the model is most optimistic. Radix-4 maximally redundant designs are predicted to be fastest, but neglect the extra latency required for 3x divisor multiple generation. Overlapped quotient selection

Architecture	$s$	$t_{int}$	$B$	$G$	$\sigma$	$t_{block}$	Bits/block	Delay/bit
$r = 2 a = 1$								
Non-overlapped	1	4.8	53	15.6	6	6.6	1	6.6
Overlap PR	2	8.4	2809	164	8	11.3	2	5.6
Overlap QS	2	6.6	106	41.2	10	9.3	2	4.6
Overlap QS	3	8.3	212	109	14	12.0	3	4.0
Overlap PRQS	2	6.0	318	153	8	8.9	2	4.4
Hybrid overlap	2	5.7	36	42.2	6	7.8	2	3.9
$r = 4 a = 2$								
Non-overlapped	1	10.6	53	15.6	6	12.4	2	6.2
Overlap PR	2	20.0	2809	164	8	22.9	4	5.7
Overlap QS	2	12.5	212	83.8	10	15.4	4	3.8
Overlap QS	3	14.3	848	449	14	18.4	6	3.1
Overlap PRQS	2	11.9	1060	515	8	15.2	4	3.8
Hybrid overlap	2	11.6	220	261	6	14.4	4	3.6
$r = 4 a = 3$								
Non-overlapped	1	9.6	53	15.9	6	11.4	2	5.7
Overlap PR	2	18.0	2809	170	8	20.9	4	5.2
Overlap QS	2	11.5	318	130	10	14.6	4	3.6
Overlap QS	3	13.5	1908	1060	14	17.8	6	3.0
Overlap PRQS	2	11.0	2226	1110	8	14.6	4	3.6
Hybrid overlap	2	10.7	420	512	6	13.9	4	3.5

**Table 6. Analytical delay model predictions**

with  $s = 3$  also appears to be faster than overlaps of just  $s = 2$  but does not account for greatly increased wire loading. Hence, choice of architecture and radix makes even less difference than the model predicts.

A potential weakness of the designs is that some have many stages and a low gain per stage. It is possible that by combining logic into fewer stages of more complex gates, speed could be improved. Suppose the number of stages could be adjusted without changing the intrinsic delay or total gain of the block. It can be shown that minimal delay occurs when the number of stages is selected to provide a gain of  $e$  per stage. This minimal delay is no more than 10% better for radix-2 designs and 5% better for radix-4 designs than the results in the table, so little benefit should be expected from combining stages.

Another interesting result of the model is that increasing parallelism does not always lead to higher speed. For example, compare overlapping either just quotient selection or both quotient selection and

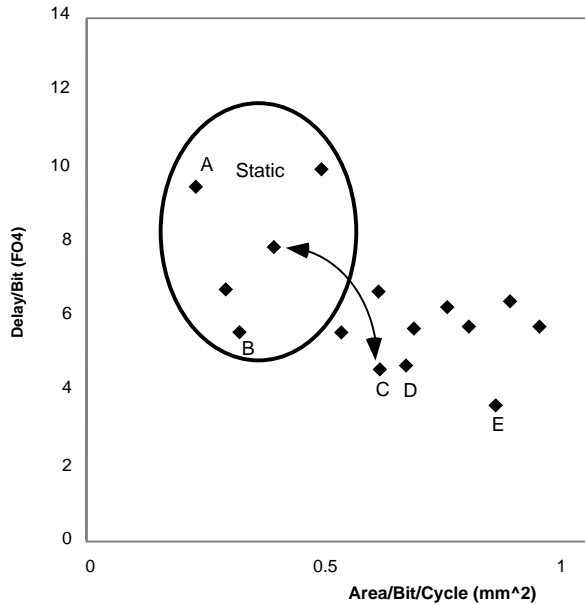


**Figure 8. Scatter plot of results**

partial remainder formation for radix-4 designs. The delays of the two designs are equal. This is because the adder delay saved by the more parallel design is lost to the higher branching effort paid to achieve this parallelism.

## 5 Simulation Results

We assigned a divider design project in an advanced VLSI circuit class at Stanford University. Twelve teams explored a wide variety of radix-2 and radix-4 double precision SRT divider designs using skew-tolerant domino circuits. The designs reflect a variety of skill levels and area/performance tradeoffs. The delay results are from HSPICE simulation, and the area estimates are based upon total transistor count and device size. We compare these results with data on static dividers extrapolated from Ercegovic [5].

The designs are shown on a scatter plot of delay/bit vs. area/bit/divider cycle, shown in Fig. 8. The labeled points are described further in Table 7 and represent those designs with the best performance for a given area. The delay/bit is measured in fanout-of-4 inverter delays in the HP-CMOS26B process. Area must be normalized by the number of bits produced per cycle because a divider can simply unroll more blocks until the cycle is full. Area is estimated in  $mm^2$  and can be converted to  $\lambda^2$  by multiplying by

Design	Architecture	$r$	$a$	$s$	Delay/bit (FO4)	Area/bit/cycle ( $mm^2$ )	QSLC Style	Notes
A	Non-overlapped	4	2	1	9.5	0.23	synthesized	smallest static
B	Hybrid overlap	4	2	2	5.7	0.33	synthesized	fastest static
C	Hybrid overlap	2	1	2	4.6	0.63	domino	most flexible
D	Overlap QS	2	1	3	4.7	0.68	domino	like UltraSparc
E	Hybrid overlap	4	3	2	3.7	0.86	1-hot PLA	fastest domino

**Table 7. Designs with best performance for given area**

$4 \times 10^6$ . Area reflects only the divider control and datapath components, not auxiliary circuits required for normalizing, rounding, and exponent handling. Design E includes the area but not the additional setup latency of a fast CPA, as maximally-redundant radix-4 designs require precomputation of the 3x divisor multiple.

The arrowheads point out two hybrid overlapped radix-2 designs. The domino design is 1.7 times as fast but has 1.6 times as much area. The extra area is attributable to generating dual-rail outputs. The fastest domino design is 1.5 times as fast as the fastest static design; radix-4 domino designs have a larger area penalty because of the larger PLA required for monotonic quotient digit selection. The skew-tolerant domino designs assume an overhead of 1 FO4 delay per 4 bits for the input mux, while static designs use 4.4 FO4 delays per 4 bits for the mux and flip-flop overhead. This is a major advantage of skew-tolerant domino circuits.

The static results from [5] were normalized with the conversion that one fanout-of-3 NAND2 delay equals 1.05 FO4 delays and has an average area of  $400 \mu m^2$ . Thus, the data for the static designs has more uncertainty than for the dynamic designs. Further, some of the static results were extrapolated from element delays tabulated in [5], rather than from complete designs. The designs in [5] assume iteration overhead of 8.4 FO4 delays in a conservative standard-cell methodology, but we use a more aggressive 4.4 FO4 delays as noted previously. The reported static quotient-selection logic delay is unexpectedly low compared with the domino.

Table 8 lists key component delays for several designs. As expected, quotient selection delay dominates the radix-4 critical path. The mux delay in design D is surprisingly low.

Design	$t_{qslc}$	$t_{mux}$	$t_{csa}$	$t_{buf}$
A,B	11.3	1.9	2.3	1.8
C	4.0	1.5	1.5	NA
D	3.6	0.9	1.5	1.1
E	7.8	1.7 - 2.6	1.7	NA

**Table 8. Selected component delays (FO4)**

For comparison, Williams [8] reports delays of overlapped quotient selection for radix-2 and radix-4 stages in terms of FO1 inverter delay. Converting these delays using  $1 \text{ FO4} \approx 2.5 \text{ FO1}$  delays, we find a delay per bit of 4.7 FO4 for radix-2 and 4.5 FO4 for radix-4. These are consistent with the delays reported in this study. Comparing area is more difficult, as Williams’ self-timed ring is constrained to overlapping of  $s = 5$  stages to hide the overhead of self-timing.

## 6 Conclusions

This study has investigated a wide range of SRT division designs. An analytical model based on the principles of logical effort allows rapid comparison of many divider architectures. The model also shows that it is essential to consider branching effort when evaluating architectures because time saved by eliminating a gate in a parallel architecture may be lost to the increased branching effort required to achieve the parallelism.

Simulation results are somewhat slower than the analytical model predicts, but still are within 20% and are consistent in their conclusions. The speed differences can be attributed to the fact that the model neglects loading from wires and from non-critical branches and that the simulations were done under time pressure and may not be thoroughly optimized.

Both the model and simulation results show that using an architecture which overlaps quotient selection improves speed, but that other overlapping details and especially the choice of either radix-2 or radix-4 make little difference in overall performance. Indeed, the architectures which the model predicts are best are also those for which the model is most optimistic. Three examples of reasonable architectures which provide high performance with modest areas are hybrid overlapped radix-2 ( $s = 2$ ), quotient



selection overlapped radix-2 ( $s = 3$ ), and hybrid overlapped maximally-redundant radix-4 ( $s = 2$ ). Although the maximally-redundant radix-4 design achieves the lowest core delay, it requires extra time and hardware outside the iterations for 3x divisor multiple generation. Also, the designs producing more bits per block ( $b \times s$ ) are less flexible, as an integral number of blocks must fit within a cycle. The reasonable architectures offer a delay/bit of 3.5-5 FO4 at a cost of approximately  $3M\lambda^2$  or 6000 transistors per bit/cycle in the core.

The choice of circuit style has a larger effect on performance. Specifically, moving from static CMOS to dual-rail domino reduces the delay of the individual gates. Skew-tolerant domino increases performance further by eliminating clocking overhead. Comparing similar architectures, dual-rail domino provides a 1.5 - 1.7x speedup over static designs. However, static designs are generally smaller than dual-rail designs of the same architecture because only one polarity of output must be generated and because quotient selection logic can be more compactly designed with non-monotonic gates. Skew-tolerant domino circuits provide the performance advantages of self-timed circuits without the complexity of asynchronous design or the need to duplicate hardware to hide control overhead. For performance-critical designs, we recommend the use of skew-tolerant dual-rail domino.

## Acknowledgments

Thanks to all of the students in EE371 for excellent work on the projects. We would like to note the designers of the “reasonable” architectures: **C** by Jeff Solomon and Derek Debusschere; **D** by Min Xu and Mengchen Yu; and **E** by Peter Richards and Peter Verplaetse. Peter Verplaetse also contributed optimized 1-hot PLA data.

This work was supported by the NSF through a fellowship and grant MIP93-13701 and by Stanford’s Center for Integrated Systems.

## References

- [1] J. E. Robertson, "A new class of digital division methods," *IRE Trans. Electronic Computers*, vol. EC-7, pp. 218–222, Sept. 1958.
- [2] K. D. Tocher, "Techniques of multiplication and division for automatic binary computers," *Quart. J. Mech. Appl. Math.*, vol. 11, pt. 3, pp. 364–384, 1958.
- [3] D. E. Atkins, "Higher-radix division using estimates of the divisor and partial remainders," *IEEE Trans. Computers*, vol. C-17, no. 10, Oct. 1968.
- [4] K. G. Tan, "The theory and implementation of high-radix division," in *Proc. 4th IEEE Symp. Computer Arithmetic*, pp. 154–163, June 1978.
- [5] M. D. Ercegovac and T. Lang, *Division and Square Root: Digit-Recurrence Algorithms and Implementations*, Kluwer Academic Publishers, 1994.
- [6] S. F. Oberman and M. J. Flynn, "Design issues in division and other floating-point operations," *IEEE Trans. Computers*, vol. 46, no. 2, pp. 154–161, Feb. 1997.
- [7] S. F. Oberman and M. J. Flynn, "Division algorithms and implementations," *IEEE Trans. Computers*, vol. 46, no. 8, pp. 833–854, Aug. 1997.
- [8] T. E. Williams and M. A. Horowitz, "A zero-overhead self-timed 160-ns 54-b CMOS divider," *IEEE J. Solid-State Circuits*, vol. 26, no. 11, pp. 1651–1661, Nov. 1991.
- [9] J. A. Prabhu and G. B. Zyner, "167 MHz radix-8 floating point divide and square root using overlapped radix-2 stages," in *Proc. 12th IEEE Symp. Computer Arithmetic*, pp. 155–162, July 1995.
- [10] S. F. Oberman, *Design Issues in High Performance Floating Point Arithmetic Units*, Ph.D. thesis, Stanford University, Nov. 1996.
- [11] M. D. Ercegovac and T. Lang, "Simple radix-4 division with operands scaling," *IEEE Trans. Computers*, vol. 39, no. 9, pp. 1204–1208, Sept. 1990.
- [12] G. S. Taylor, "Radix 16 SRT dividers with overlapped quotient selection stages," in *Proc. 7th IEEE Symp. Computer Arithmetic*, pp. 64–71, June 1985.
- [13] N. Quach and M. Flynn, "A radix-64 floating-point divider," Technical Report No. CSL-TR-92-529, Computer Systems Laboratory, Stanford University, June 1992.
- [14] J. Fandrianto, "Algorithm for high-speed shared radix 8 division and radix 8 square root," in *Proc. 9th IEEE Symp. Computer Arithmetic*, pp. 68–75, July 1989.
- [15] H. P. Sharangpani and M. L. Barton, "Statistical analysis of floating point flaw in the pentium processor," Intel Corporation White Paper, November 1994.

- [16] P. Gronowski et al., “A 433-MHz 64-b quad-issue RISC microprocessor,” *IEEE J. Solid-State Circuits*, vol. 31, no. 11, pp. 1687–1696, Nov. 1996.
- [17] D. Harris and M. Horowitz, “Skew-tolerant domino circuits,” *IEEE J. Solid-State Circuits*, vol. 32, no. 11, pp. 1702–1711, Nov. 1997.
- [18] T. Asprey, G. S. Averill, E. DeLano, R. Mason, B. Weiner, and J. Yetter, “Performance features of the PA7100 microprocessor,” *IEEE Micro*, vol. 13, no. 3, pp. 22–35, June 1993.
- [19] I. E. Sutherland, R. F. Sproull, “Logical Effort: Designing for Speed on the Back of an Envelope,” in *Proc. 1991 Conference on Advanced Research in VLSI*, pp. 1–16, March 1991.